Journal of Power Sources 192 (2009) 94–99

Contents lists available at ScienceDirect

Journal of Power Sources

journal homepage: www.elsevier.com/locate/jpowsour

Comparison of water management between two bipolar plate flow-field geometries in proton exchange membrane fuel cells at low-density current range

Ana M. López, Félix Barreras*, Antonio Lozano, Juan A. García, Luis Valiño, Radu Mustata

LITEC, CSIC-Univ. Zaragoza, Maria de Luna 10, 50018, Zaragoza, Spain

ARTICLE INFO

Article history:
Received 3 October 2008
Received in revised form 1 December 2008
Accepted 16 December 2008
Available online 27 December 2008

Keywords:
PEM fuel cells
Bipolar plate geometries
Water management
Water buildup

ABSTRACT

This experimental research studies some aspects of water formation and management in polymer electrolyte membrane fuel cells (PEMFCs). To this end, two different single cells of 49 cm^2 active area have been tested, the first one with a serpentine-parallel geometry and the second with a cascade-type flow-field topology. In order to visualize the processes, flow-field channels have been machined on transparent plastic. Experiments have consisted in both image acquisition using a CCD camera, and simultaneous measurements of pressure drop in both hydrogen and oxygen gas flow paths. It has been observed that with the cascade-type flow-field geometry, water produced in the cathode does not flood the gas flow channels and, consequently, can be drained in an easy way. On the other hand, it has also been verified that saturated condition for the hydrogen gas flow at the anode side produces water condensation and channel flooding for the serpentine-parallel flow-field topology. Time fluctuations in the pressure drop of the gas flow have been detected and are associated to some transient process inherent to water formation and management.

1. Introduction

Water management in low-temperature PEMFC is a key process in the performance of these electrochemical devices. If the water inside the cell is insufficient, the membrane polymer dries out increasing the resistance to proton transport, drastically reducing the efficiency. Water balance of a hydrogen-fueled PEMFC is related to several mechanisms. Due to electro-osmotic drag in the membrane, water supplied to the electrodes by humidification of the reactant gases tends to migrate from anode to the cathode. On the other hand, the formation of water by the electrochemical reactions causes the water concentration in the cathodes to be higher than in the anodes. Due to this concentration gradient, there is a back-diffusion from cathode to anode through the polymeric membrane, intensified by the pressure difference imposed to the gases. Finally, water produced by species recombination at the cathode side has to be continuously extracted; otherwise it will flood the very small pores in the GDL hindering the transport of gases to the reaction zones. This process becomes critical when the PEM fuel cell is operated at high current density ranges, causing oxygen starvation to the catalyst layers, eventually stopping the power generation.

Water management has been the subject of many experimental and theoretical studies in the last few years. Focusing on the experimental point of view, several techniques have been used, as magnetic resonant imaging [1,2], neutron radiography [3,4], residence time distribution [5,6], and direct water visualization in transparent plates [7–13]. Most of the previous studies based on direct visualization in transparent cells, have analyzed the effect of the diffusion layer characteristics on the water generated in the cathode side using standard [7,8] or suitable modified [7,9] gas diffusion layers (GDLs), but all of them using bipolar plates with serpentine or parallel channel flow-field geometries. A recent study [13] has compared the performance of different commercially available GDL materials in a 10 cm^2 single-serpentine PEMFC under "realistic" operating conditions. Even when visualization results of water buildup and transport obtained from transparent fuel cell experiments have some limitations due to the distortion of both temperature and current distribution when non-conducting plates are used [14], this technique can be applied and results are reliable when the fuel cells are operated at low-current density values.

The objective of this work has been to analyze the influence of two different bipolar plate flow-field geometries, namely a parallel-serpentine, and a cascade-type, on water formation and management. The 49 cm^2 active area plates have been machined on transparent methacrylate. To extract the electrons allowing the suitable electrochemical performance of the cells, two copper collecting plates have been placed just over the channel ribs. The same polymer electrolyte membrane, carbon cloth GDL and catalyst concentration have been used in the MEAs for the two cells. At the same time, fixed hydrogen and oxygen gas flow conditions have been established in order to guarantee the low-current density

* Corresponding author. Tel.: +34 976 716 30; fax: +34 976 716 456.
E-mail address: felix@litec.csic.es (F. Barreras).

0378-7753/$ – see front matter © 2008 Elsevier B.V. All rights reserved.
doi:10.1016/j.jpowsour.2008.12.082

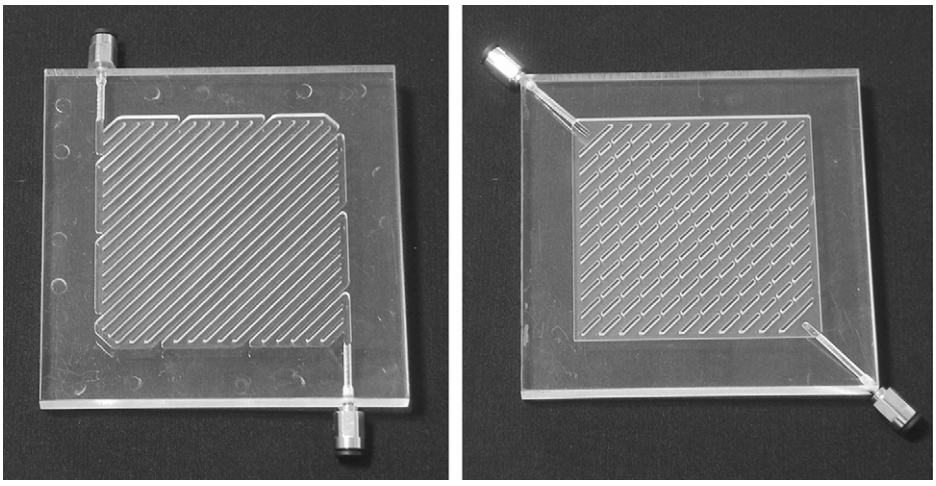

Fig. 1. Photographs of the two flow-field topologies: (a) serpentine-parallel channels, and (b) cascade-type geometry.

range for the cells. Besides the comparison of the two flow-field geometries, another interest of this experimental research has consisted in the simultaneous analysis of image sequences acquired for the anode and cathode sides, and the measurement of the pressure drop in both hydrogen and oxygen gas flow paths, as strongly recommended and performed in previous studies [7,14].

2. Experimental facilities

As shown in Fig. 1, two different flow-field geometries have been tested in this work, a serpentine-parallel and a cascade-type. These two geometries have been selected taken into account results from previous fluid dynamics analysis [15,16]. It was observed that the serpentine-parallel geometry provides a very homogeneous velocity field but with relatively large pressure differences across the plate active area, which can result in a defective gas distribution after the GDL. On the contrary, the cascade-type flow-field yields a smooth pressure field and a very uniform gas flow distribution over the catalyst layers. The two plate geometries have some common dimensions, for example, an active area of 7 cm × 7 cm, diameter of inlet and outlet ducts of 2 mm, and depth of the channels of 1 mm. Unlike most parallel-serpentine plates, in which the set of channels are displaced parallel to the two edges of the flow area, the serpentine-parallel plates in this work depicted in Fig. 1(a), have a diagonal distribution similar to that in the cascade design, arranging the 1-mm wide 32 channels in 11 blocks. In this case, inlet and outlet ports have been located in suitable positions to ease the experimental assembly and the fluid flow. The cascade flow-field bipolar plates shown in Fig. 1(b) consist of 20 longitudinal channels 3.1-mm wide, separated by ribs with a thickness of 1 mm. In this last configuration the perpendicular flow area connecting one channel to the next one has been maintained constant and equal to the cross-sectional area of the inlet duct. So, the number and width of the slits on each rib change from one to the other. Push-in quick connectors have been placed at inlet and outlet ports to ease the assembly to gas pipes.

To allow the correct electrochemical performance of the cells, two copper-metal frames have been superimposed and glued to the plastic machined plates, providing the needed electrical contact between the MEA and the ribs of the end-plates. Anode and cathode plates have been assembled using U-shaped stainless steel profiles with three M6 screws, placed in each edge of the cells as depicted in Fig. 2 for the cascade-type plates. To ensure the adequate gas tightness of the system, two silicone-based soft seals 0.5-mm thick have been used. Compressed hydrogen (Air Liquide AlphaGaz 1 with a global purity of 99.999%) and industrial oxygen have been supplied to the cells from two B50-type bottles. The volumetric flow rate of the reactant gases, considering stoichiometric ratios of 1.5 and 2.0 for both hydrogen (56.7 ml min^{-1}) and oxygen (37.4 ml min^{-1}) gas flows, have been controlled with two rotameters. During the experiments, gases were supplied to the single cells at a temperature of 60 °C and fully humidified by bubbling them into pure water.

Each membrane-electrode assembly has been manufactured using commercially available products. Nafion® 1035 89-μm thick perfluorinated ion-exchange membrane has been used as electrolyte. Prior to use, the membrane was treated, boiling it in both hydrogen peroxide and 1 M sulfuric acid solutions to fully convert it to the H^+ form. After the treatment, a catalytic layer has been sprayed on the two sides of the membrane forming the electrodes. For the preparation of the ink, the required quantity of a 40 wt.% Pt electrocatalyst supported on Vulcan XC-72, purchased to BASF Fuel Cell Inc., has been ultrasonically mixed with a solution formed by 99.8% isopropyl alcohol, pure water, and 5 wt.% Nafion® perfluorinated resin solution, in order to apply a catalyst load of 0.7 mgPt cm^{-2} for the cathode, and 0.3 mgPt cm^{-2} for the anode. Catalyst ink was directly sprayed onto the membrane using a commercial airbrush. Finally, to form the 5-layer MEA, the gas diffusion layers and the catalyst-deposited membranes have been assembled by hot-pressing. In this case an E-Tek proprietary carbon cloth 350-μm thick with a 10% of Teflon has been used as gas diffusion media. The carbon cloths and the deposited membrane have been pressed during 5 min at 120 bar and at a temperature of 75 °C. Good adherence results have been obtained.

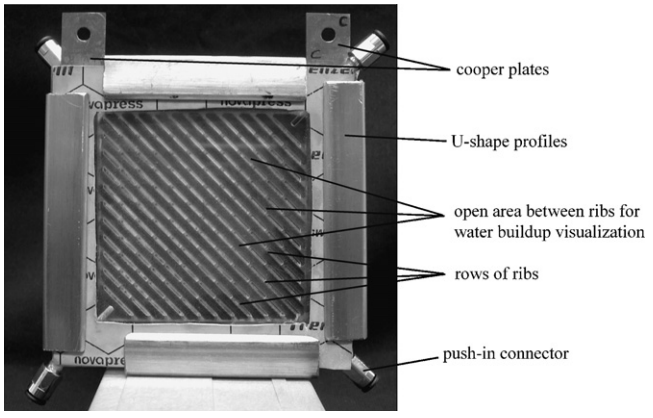

Fig. 2. Picture of the cascade-type plate assembled fuel cell, highlighting its different parts.

To provide an electric load to the fuel cells, anode and cathode copper-plates have been connected to the terminals of a decade resistor box, with a minimum value of 0.01 Ω. In order to minimize the distortions caused by the use of plastic bipolar plates, with very low thermal and electric conductivities, the fuel cells have been operated at low-current values (below 0.1 A cm^{-2}) adjusting the load resistance. During the experiments both voltage and current have been constantly monitorized (although not recorded).

Water evolution in both cathode and anode has been visualized through the open area between the different rows of ribs (see Fig. 2). To record the images, an interlined Hamamatsu ORCA-ER 1024 × 1024 pixels CCD camera has been used, placed perpendicular to the bipolar plate to avoid any perspective distortion. Data sets have been acquired with a 50 mm f#1.2 Nikon lens, with a field of view of 100 mm × 100 mm and a spatial resolution of 97.6 μm pixel^{-1}. In order to analyze the influence of the water deposited in the gas flow channels on the gas supply system, pressure drop in both hydrogen and oxygen flow paths has also been measured, simultaneously to the image acquisition. To this end, the two branches of two differential inclined-tube manometers have been connected to the inlet and outlet ducts at cathode and anode sides. Due to the small pressure difference measured especially at low volumetric flow rates, a 15° inclination angle has been used in order to increase the differential reading by a factor of 3.86 ($1/\sin\theta$).

3. Results

Results obtained when measuring the pressure drop for both flow-field geometries for different volumetric flow rates without chemical reaction are depicted in Fig. 3. As it can be observed, the difference is always higher in the serpentine-parallel configuration than in the cascade-type one, even for low volumetric gas flow rates. These results indicate that a power unit consisting of a fuel cell stack made of bipolar and end plates with the serpentine-parallel flow-field geometry will have a lower overall efficiency due to the excess energy consumed for the gas supply system.

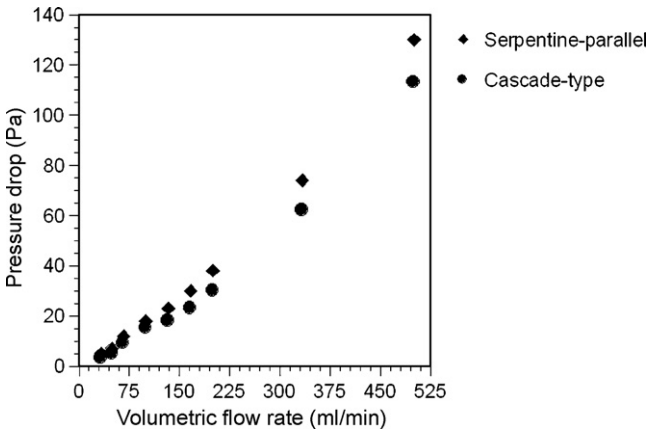

Fig. 3. Pressure drop measured for the two types of geometries for different volumetric flow rates.

With the selected load resistance the maximum current produced by the cells has been 3.5 A, maintaining a nearly constant value. In the same way, the measured voltage for the two cells was stabilized during the tests to an almost constant value of 0.25 V, independently of the water behavior inside them. It is to be noted that with the difficulties in controlling the temperature, the tested cells have yielded lower efficiencies than the typical ones for these

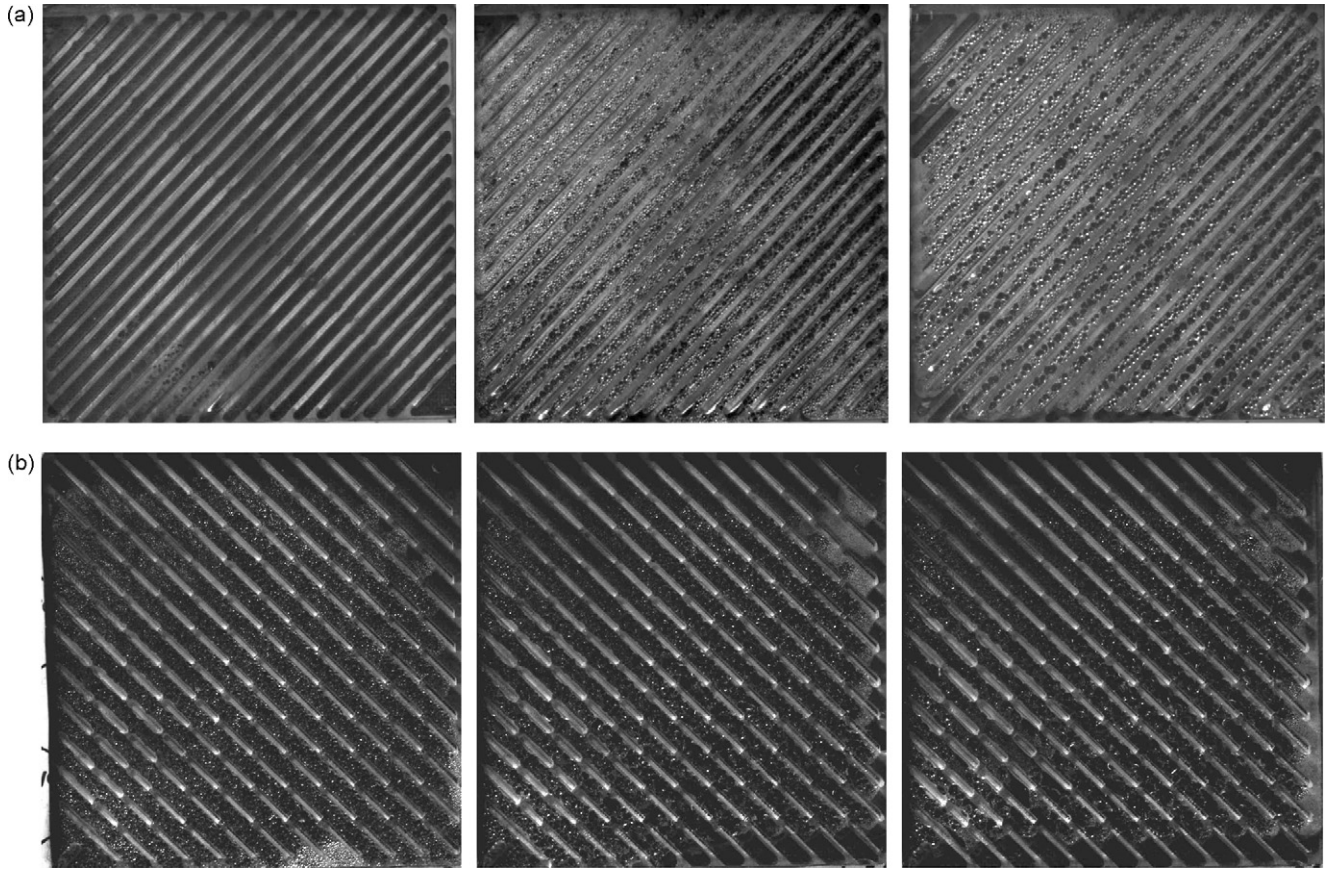

Fig. 4. Images of the water buildup at the cathode side corresponding to 20, 60, and 100 min after the beginning of the experiments for both (a) serpentine-parallel and (b) cascade-type geometry.

devices. In any case, the main objective of this work has been to compare the performance of the two plate geometries under the same operating conditions even if they were not optimal.

3.1. Cathode side water buildup and management

In order to ease the interpretation of the results, all the experiments have been performed with open anode and cathode exit ports, to minimize water transport through the membrane by pressure gradients. A sequence of images of the formation and behavior of water at the cathode side is shown in Fig. 4 for both the serpentine-parallel (a) and the cascade-type (b) flow geometries, corresponding to 20, 60, and 100 min after the start-up of the cells. It can be concluded that even when the oxygen flow is saturated, the main fraction of the water observed in the cathode side is produced by chemical reaction, because no water condensation at the entrance or big water droplets occluding the channels have been observed. On the contrary, a dense mist of very small droplets is produced at given areas, and eventually deposited over the plate surfaces. The large amount of liquid water condensed (bright areas in the pictures) is enhanced by both the experimental procedure followed in the study, and the use of plastic bipolar plates, even when low current is produced by the cells. On the one hand, after the conditioning steps, the cells have been switched from open circuit to 3.5 A by connecting the appropriate load resistor. This abrupt change in the operational conditions caused a fine mist to be formed almost instantaneously. Besides, water condensation on the plates is increased because plastic has a very low thermal conductivity keeping its temperature close to room conditions. A metal plate, for example, would heat up in a short time due to the heat released by chemical reaction, reducing the condensation on its surface.

It has been verified that the amount of water observed inside the cell during the duration of the test was higher in the serpentine-parallel geometry than in the cascade one. As can be seen in Fig. 4(a), the large amount of water condensed in the plate surface of the serpentine-parallel geometry could flood the gas distribution channels, and, for the present experimental conditions of low oxygen flow rate, the reactant gas pressure might be too low to drag it. Of course, this scenario causes a reduction in the fuel cell efficiency, limiting the gas flow circulation, and, as a consequence, the total reacting area. On the other hand, a low concentration of droplet mist over the transparent plate surface, and no water dragging by gas flow in any channel of the cascade-type flow-field geometry have been detected. The particular design of this plate enhances the draining of condensed water by the lateral channels, as can be observed in the image sequence depicted in Fig. 4(b). However, the positioning of the cells with the bottom channel parallel to the floor allows the accumulation of water in it. This result suggests that if these plates are placed slightly rotated, trying to place the exit ports perpendicular to the floor the extraction of water can be further improved.

The main results derived from the analysis of the acquired images are also supported by the behavior of the pressure drop along the gas flow paths. It has been observed that, a few minutes after the beginning of the experiments, pressure drop increases gradually until a constant value is reached, caused by the water produced by chemical reaction in the cathode side. In the case of the serpentine-parallel flow-field cell the pressure drop increase rises from 20 to 50 Pa, while for the cascade-type cell it varies from 15 to 30 Pa. As the current density remained constant for the two cells during the whole experiment, this behavior suggests that the cathode gas diffusion layers could be partially flooded few

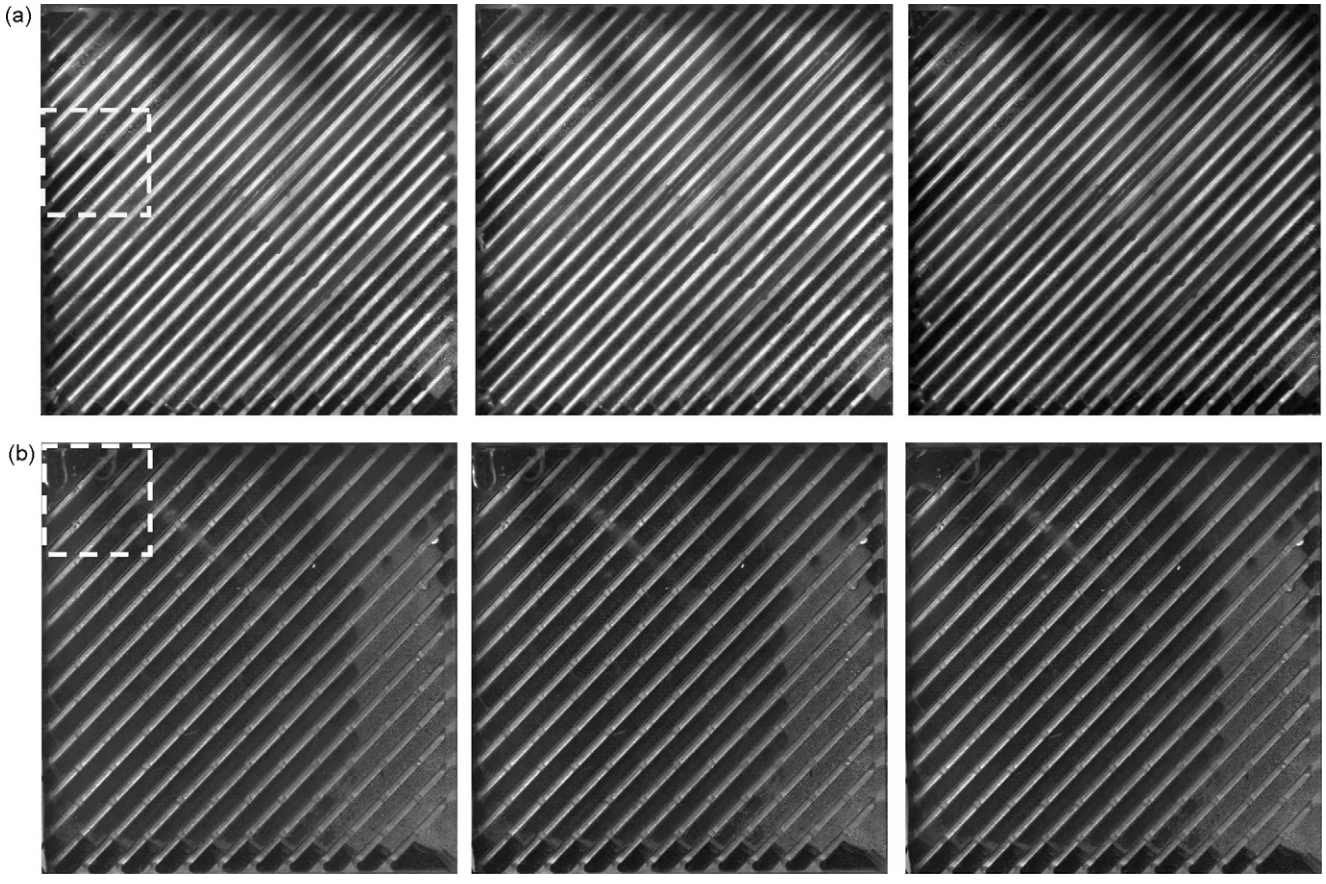

Fig. 5. Water behavior in three consecutives images acquired 45 min after the start-up of the cells for both (a) the serpentine-parallel and (b) cascade-type flow-field.

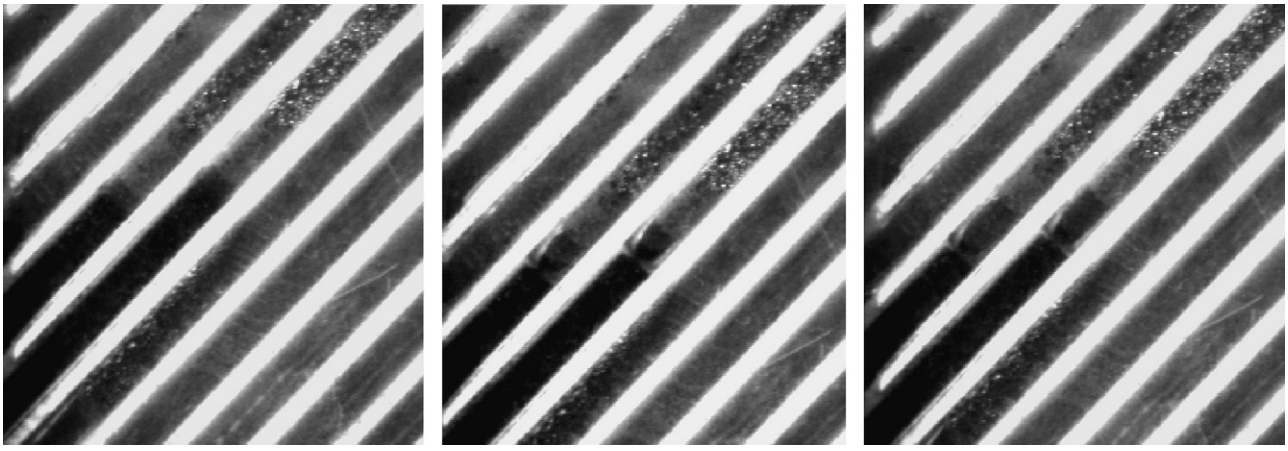

Fig. 6. Image sequences of the water meniscus formed in two channels of the serpentine-parallel geometry due to the gaseous flow drag. Images correspond to a zoom of the marked area in Fig. 5(a).

minutes after the start of the cells operation. All these results indicate that the water generated by chemical reaction is, at least for these experimental conditions, better managed by plates with a cascade-type flow-field topology than for those with serpentine-parallel channels. It should be noted that due to the particular plate design that keeps constant the cross-sectional flow area, the gas flow also maintains a constant velocity in every row of ribs [15]. After crossing the ribs the gas is forced to fill the whole open area favoring its flow through the GDL towards the catalyst layers. The excellent gas distribution over the catalyst layer for the cascade-type plates has been previously demonstrated [16] for a non-reacting cell.

3.2. Water behavior at the anode side

The water visualized at the anode side is originated only from the hydrogen humidity, as the experiments have been performed with open anode and cathode exit ports, neglecting the water transport through the membrane by pressure gradients. A sequence of three consecutive images corresponding to both the serpentine-parallel, and the cascade-type single cells are depicted in Fig. 5(a and b). Images have been acquired 45 min after the start-up of the cells, and the time interval between each one is 5 s. In all images the inlet hydrogen port is placed at the top-left corner, and the exit one at the lower-right corner. In general, when saturated hydrogen enters the fuel cell, a sudden expansion occurs. This fact combined with the low (room) temperature of the plates cause the water condensation. As can be seen, the large bright region of Fig. 5(a) corresponds to an increase in the light scattered by the droplets of water accumulated over the plate. This result suggests a worse water drag and management for the serpentine-parallel flow-field configuration. It is also notorious the amount of water accumulate in the bottom part of the plate. For this flow-field geometry, a large pressure drop is imposed to the gas flow circulation due to the partial, or total, blockage of several channels. As described in other references (see, for example [9]), there are several patterns for the drag of liquid water inside a channel: homogeneous two-phase flow, corner flow, annular film flow, and slug flow. When individual water droplets emerge from the catalyst layer to the external side of the GDL, they tend to be dragged and deposited onto the channel walls causing either corner or annular flows. However, if water accumulates, especially in narrow channels, it can block them, resulting in a slug flow pattern that requires higher gas pressure and velocity to evacuate the liquid and maintain the gas flow. In the case of the cascade-type geometry fuel cell, the specific design of this plate geometry allows the drain of the condensed water through the lateral channels avoiding the flooding of the reacting zones in the central part of the plates, as can be observed in Fig. 5(b). Again, the drained water from channels accumulates at the bottom of the plate, but if the plate is arranged with the exit ports perpendicular to the floor, the extraction of the water produced could be easily improved.

Transient characteristics of the water condensation and transport processes will be discussed looking at the small zoomed in areas marked in Fig. 5(a) and (b). Results are depicted in Figs. 6 and 7. In the case of the serpentine-parallel plate the presence of a water meniscus in some gas flow channels can be observed, as shown in Fig. 6. The growing of the meniscus in the two central channels of the sequence due to the drag of the hydrogen flow can be easily detected. When the drag force of the gas flow exceeds the surface tension force, breakup of the liquid interface occurs. This process is repeated in time in several different channels. On the other hand, for the cascade-type geometry a droplet of water is formed just at the inlet port, as indicated in Fig. 7. The sequence of images shows that the droplet grows and quickly falls down due to gravity. These observations are in good agreement with the pressure drop measurements. Some fluctuations around the steady value of this parameter have been verified for the two plate geometries. For the time corresponding to the images in Figs. 6 and 7 (45 min), a steady pressure drop of 60 Pa has been measured for the serpentine-parallel flow-field geometry, compared to 40 Pa for the cascade-type one. A first increase to around 140 Pa is detected for the serpentine-parallel cell, which could correspond to the instant just before the breakup of the liquid meniscus inside the channels caused by the dragging gas flow. After that, the pressure drop is again stabilized, close to the steady value. These observations are also indicative of a sustained slug flow along the plate channels, opposite to an annular flow that would be preferable [9]. These conditions could be improved by modifying the channel width, but the main objective is not to optimize the serpentine-parallel design, but to compare it with a completely different concept, the cascade type. For this latter plate design, as the breakup of the droplet formed at the entrance is also assisted by the gravity force, the increase in measured pressure drop only reached 98 Pa before the re-stabilization around the steady value. To the authors' knowledge, a discussion about pressure drop fluctuations on the gas flow system due to transient processes associated to water formation and management has never been reported before. However, gas flow fluctuations might be beneficial for a PEM fuel cell performance as they can increase diffusion up to three or four orders of magnitude

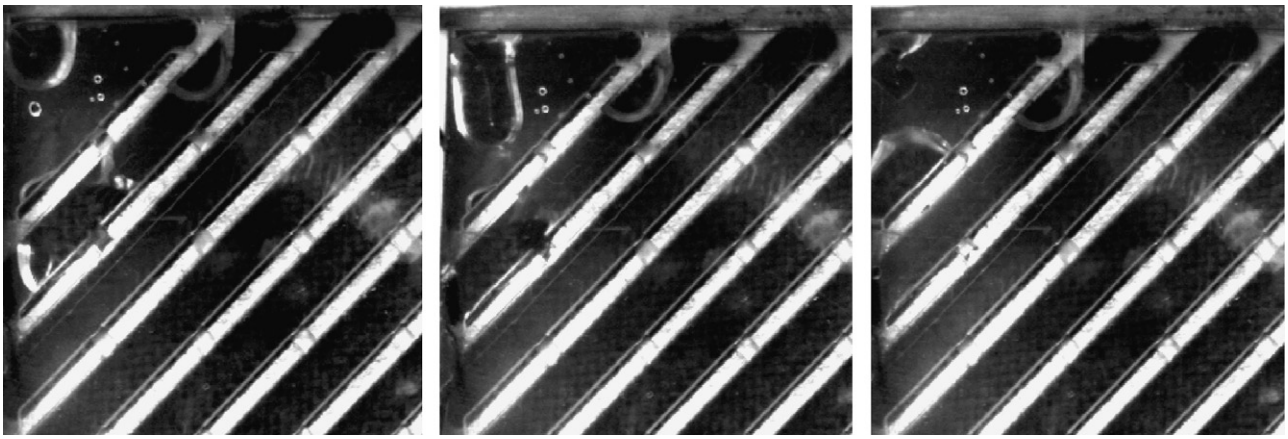

Fig. 7. Formation and breakup of a water droplet at the inlet channel of the cascade-type flow-field geometry. Images correspond to a zoom of the marked area in Fig. 5(b).

above the molecular diffusion coefficient [17], as recently demonstrated by acoustically forcing the gas flow in the cathode side of a single cell [18].

4. Conclusions

This experimental research on water formation, condensation and management based on flow visualization, image analysis and pressure drop measurements for two different flow-field geometries, has revealed some important features for both anode and cathode sides. As expected, most of the water observed at the cathode side is produced by chemical reaction. In this zone, a dense mist of very small droplets is produced at given areas, and eventually deposited over the plate surfaces. It has been verified that the amount of water observed inside the cells at the end of the test was higher for the serpentine-parallel geometry than for the cascade-type one. This result is in good agreement with the different measured increase in the pressure drop for the two flow-field geometries, and suggests that the water produced by chemical reaction is better managed by plates with a cascade-type flow-field topology than by those with serpentine-parallel ones. With the relative humidity selected for the reactant gases in these experiments, close to 100%, water condensation occurs at the entrance of the anode sides. In them, channel flooding has been observed for the serpentine-parallel flow-field geometry. Fluctuations in the pressure drop of the gas flow have been verified and they are associated to some transient process inherent to water formation and management. Causes are different for the two flow-field geometries studied. For the case of the serpentine-parallel topology, pressure drop fluctuations can be produced by the dragging and breakup of the water meniscus in the gas flow channels. Droplet growing and breakup could be the responsible for this behavior in the cascade-type bipolar plate geometry. The suitable design of the gas circulation channels and the positioning of the lateral ones in the cascade-type flow-field plates allow the fast drainage of water condensed over the plates without flooding the active area in the center part of the cells. In the future, the benefits of the cascade-type flow filed geometry on the performance of PEMFC will be tested in cells operating in the high current density range.

Acknowledgements

This research has been partially funded by the Spanish Ministry of Education and Science under projects ENE2005-09124-C04-03/ALT, and ENE2007-68071, and by the Aragón Regional Government under project PM042/2007.

References

[1] V.R. Albertini, B. Paci, A. Generosi, S. Panero, M.A. Navarra, M. di Michiel, Electrochemical and Solid State Letters 7 (2004) A519–A521.
[2] P.K. Sinha, P. Halleck, C.Y. Wang, Electrochemical and Solid State Letters 9 (2006) A344–A348.
[3] A.B. Geiger, A. Tsukada, E. Lehmann, P. Vontobel, A. Wokaun, G.G. Sherer, Fuel Cells 2 (2002) 92–98.
[4] N. Pekula, K. Heller, P.A. Chuang, A. Turhan, M.M. Mench, J.S. Breziner, K. Ünlü, Nuclear Instruments and Methods in Physics Research A 542 (2005) 134–141.
[5] J. Diep, D. Kiel, J. St-Pierre, A. Wong, Chemical Engineering Science 62 (2007) 846–857.
[6] J. St-Pierre, A. Wong, J. Diep, D. Kiel, Journal of Power Sources 164 (2007) 196–202.
[7] K. Tüber, D. Pócza, C. Hebling, Journal of Power Sources 124 (2003) 403–414.
[8] A. Hakenjos, H. Muenter, U. Wittstadt, Ch. Hebling, Journal of Power Sources 131 (2004) 213–216.
[9] F.Y. Zhang, X.G. Yang, C.Y. Wang, Journal of the Electrochemical Society 153 (2006) A225–A232.
[10] K. Sugiura, M. Nakata, T. Yodo, Y. Nishiguchi, M. Yamauchi, Y. Itoh, Journal of Power Sources 145 (2005) 526–533.
[11] X. Liu, H. Guo, C. Ma, Journal of Power Sources 156 (2006) 267–280.
[12] Y. Ishikawa, T. Morita, K. Nakatab, K. Yoshida, M. Shiozawa, Journal of Power Sources 163 (2007) 708–712.
[13] D. Spernjak, A.K. Prasad, S.G. Advani, Journal of Power Sources 170 (2008) 334–344.
[14] J. St-Pierre, Journal of the Electrochemical Society 154 (2007) B724–B731.
[15] F. Barreras, A. Lozano, L. Valiño, R. Mustata, C. Marín, Journal of Power Sources 175 (2008) 841–850.
[16] A. Lozano, L. Valiño, F. Barreras, R. Mustata, Journal of Power Sources 179 (2008) 711–722.
[17] U.H. Kurzweg, Journal of Fluid Mechanics 156 (1985) 291–300.
[18] Y.H. Kim, H.S. Han, S.Y. Kim, G.H. Rhee, Journal of Power Sources 185 (2008) 112–117.